Original Article
Yonsei Med J 2015 Nov;56(6):1538-1544
http://dx.doi.org/10.3349/ymj.2015.56.6.1538
Yonsei Medical Journal
YMJ
pISSN: 0513-5796 · eISSN: 1976-2437

Impact of Coronary Plaque Characteristics on Late Stent Malapposition after Drug-Eluting Stent Implantation

Sung-Jin Hong[1*], Byeong-Keuk Kim[2,3*], Dong-Ho Shin[2,3], Jung-Sun Kim[2,3], Young-Guk Ko[2,3], Donghoon Choi[2,3], Yangsoo Jang[2,3,4], and Myeong-Ki Hong[2,3,4]

[1]Division of Cardiology, Department of Internal Medicine, Sanggye Paik Hospital, Inje University College of Medicine, Seoul;
[2]Division of Cardiology, Severance Cardiovascular Hospital, Yonsei University College of Medicine, Seoul;
[3]Cardiovascular Institute, Yonsei University College of Medicine, Seoul;
[4]Severance Biomedical Science Institute, Yonsei University College of Medicine, Seoul, Korea.

Purpose: To evaluate the impact of pre-procedural coronary plaque composition assessed by virtual histology intravascular ultrasound (VH-IVUS) on late stent malapposition assessed by optical coherence tomography (OCT) following drug-eluting stent (DES) implantation.

Materials and Methods: The study population consisted of 121 patients (121 lesions) who underwent both pre-procedural VH-IVUS and follow-up OCT after DES implantation. The association between pre-procedural plaque composition [necrotic core (NC), dense calcium (DC), fibrotic (FT), and fibro-fatty (FF) volumes] assessed by VH-IVUS and late stent malapposition (percent malapposed struts) or strut coverage (percent uncovered struts) assessed by follow-up OCT was evaluated.

Results: Pre-procedural absolute total NC, DC, FT, and FF plaque volumes were 22.9±19.0, 7.9±9.6, 63.8±33.8, and 16.5±12.4 mm^3, respectively. At 6.3±3.1 months post-intervention, percent malapposed and uncovered struts were 0.8±2.5% and 15.3±16.7%, respectively. Pre-procedural absolute total NC and DC plaque volumes were positively correlated with percent malapposed struts (r=0.44, p<0.001 and r=0.45, p<0.001, respectively), while pre-procedural absolute total FT plaque volume was weakly associated with percent malapposed struts (r=0.220, p=0.015). Pre-procedural absolute total DC plaque volume was the only independent predictor of late stent malapposition on multivariate analysis (β=1.12, p=0.002). There were no significant correlations between pre-intervention plaque composition and percent uncovered struts.

Conclusion: Pre-procedural plaque composition was associated with late stent malapposition but not strut coverage after DES implantation. Larger pre-procedural absolute total DC plaque volumes were associated with greater late stent malapposition.

Key Words: Drug-eluting stent, intravascular ultrasound, optical coherence tomography

INTRODUCTION

Given concerns regarding late drug eluting stent (DES) thrombosis, imaging modalities have attempted to identify risk factors for the occurrence of stent thrombosis.[1-4] Of these, late stent malapposition or incomplete coverage of stent struts after DES implantation have been suggested as major potential risks for late adverse clinical outcomes, such as late stent thrombosis.[1-5] Additionally, several clinical and procedural features after DES implantation have been postulated as potential risk factors for late stent malapposition and incomplete coverage of stent struts. Optical coherence tomography (OCT) has been used to evaluate these risk factors due to its superior resolution over other imaging modalities.[4,6,7] Nevertheless, little data exists regarding the impact of plaque characteristics or composition of *de novo* lesions on vascular healing responses, particularly late stent malapposition or incomplete strut cov-

Received: September 3, 2014 **Revised:** November 18, 2014
Accepted: December 23, 2014
Corresponding author: Dr. Myeong-Ki Hong, Division of Cardiology, Severance Cardiovascular Hospital, Yonsei University College of Medicine, 50-1 Yonsei-ro, Seodaemun-gu, Seoul 03722, Korea.
Tel: 82-2-2228-8458, Fax: 82-2-393-2041, E-mail: mkhong61@yuhs.ac

*Sung-Jin Hong and Byeong-Keuk Kim contributed equally to this work.
•The authors have no financial conflicts of interest.

erage, after DES implantation.[8-10]

We hypothesized that quantitative assessment of plaque composition could predict late stent malapposition or incomplete strut coverage after DES implantation. We sought to prove this hypothesis by evaluating the association between pre-procedural coronary plaque composition on virtual histology intravascular ultrasound (VH-IVUS) and strut malapposition or coverage on follow-up OCT after DES implantation.

MATERIALS AND METHODS

Between July 2010 and December 2011, we identified 121 eligible patients (121 lesions) who underwent both pre-procedural VH-IVUS examination on *de novo* lesions and follow-up OCT after DES implantation from an OCT registry database at our institute. Patients or lesions with the following characteristics were excluded from this study: 1) untreated significant left main coronary artery disease, bifurcation treated with two-stent techniques, in-stent restenosis, graft stenosis, or overlapping DES; 2) ST-elevation myocardial infarction; 3) hemodynamically unstable status or ejection fraction <30%; 4) renal insufficiency with baseline creatinine ≥2.0 mg/dL; and 5) poor intravascular ultrasound (IVUS) or OCT image quality. This study protocol was approved by the Institutional Review Board of Yonsei University College of Medicine. All patients provided written informed consent.

DESs were selected by operators at the time of implantation and included sirolimus-eluting stents (Cypher, Cordis, Miami, FL, USA), zotarolimus-eluting stents (Resolute or Integrity, Medtronic, Santa Rosa, CA, USA), everolimus-eluting stents (Xience, Abbott Vascular, Santa Clara, CA, USA), or biolimus A9-eluting stents (Nobori, Terumo Corporation, Tokyo, Japan or Biomatrix, Biosensors International, Singapore). Each DES was implanted with conventional techniques. Unfractionated heparin was administered as an initial bolus of 100 IU/kg, with additional boluses administered during the procedure to achieve an activated clotting time of 250 to 300 seconds. Dual antiplatelet therapy (aspirin and clopidogrel) was prescribed at least until the follow-up OCT was performed. Quantitative coronary angiography analyses were performed before and after stent implantation and at follow-up using an off-line quantitative coronary angiographic system (CASS system, Pie Medical Instruments, Maastricht, the Netherlands) in an independent core laboratory (Cardiovascular Research Center, Seoul, Korea). Reference vessel diameters and minimal luminal diameters were measured with a guiding catheter for magnification-calibration from diastolic frames in a single, matched view that showed the smallest minimal luminal diameter.

The VH-IVUS examination was performed in the target lesion before pre-dilation using a 20-MHz 2.9 Fr, phased-array IVUS catheter (Eagle Eye, Volcano Therapeutics, Rancho Cordova, CA, USA). After intracoronary administration of nitroglycerin (200 μg), the IVUS catheter was placed distal to the target lesion and then pulled back using a motorized pullback system at 0.5 cm/s. During pullback, gray-scale IVUS was recorded, and raw radiofrequency data were captured at the top of the R wave for reconstruction of a color-coded map by a VH-IVUS data recorder (Volcano Therapeutics). Gray-scale quantitative IVUS analyses of the external elastic membrane, lumen, and plaque and media (external elastic membrane-lumen) were performed according to the Clinical Expert Consensus Document on IVUS.[11] VH-IVUS data were analyzed for the entire length of the target lesion covered by DES with 1-mm intervals for volumetric analysis. On the pre-procedural IVUS images, the diseased segment was selected and the references were defined as the most normal-appearing segments within 5 mm proximal and distal to the lesion shoulders. Also, the region of interest, matched frames of the stented segment on follow-up OCT images, was identified based on anatomic landmarks, such as side branches or calcification, aided by angiographic images revealing the IVUS catheter position. VH-IVUS analysis coded tissue as red (necrotic core, NC), white (dense calcium, DC), green (fibrotic, FT), or yellow-green (fibro-fatty, FF).[12,13] The findings of VH-IVUS analyses were described as absolute volumes and percentages (relative amounts) of plaque volumes.

OCT was performed using two OCT systems (Model M2 Imaging System and C7-XR Imaging System, LightLab Imaging, Inc., St. Jude Medical, St. Paul, MN, USA).[6,9] All of the OCT images were analyzed at a core laboratory (Cardiovascular Research Center, Seoul, Korea) by analysts who were blinded to patient and procedural information. Cross-sectional OCT images were analyzed at 1-mm intervals. Stent and luminal cross-sectional areas (CSA) were measured, and neointimal hyperplasia (NIH) CSA was calculated as the stent CSA minus the luminal CSA.[6] Total stent, lumen, and NIH volumes within stented segments were calculated. NIH thickness, which was the distance between the endoluminal surface of the neointima and the strut, was measured inside each strut with a line perpendicular to the neointima and strut.[14] An uncovered strut was defined as having a NIH thickness of 0 μm.[7,14,15] Stent malapposition was defined as the presence of any malapposed struts.[15-17] A malapposed strut was defined as a strut that was detached from the vessel wall as follows: Cypher, ≥160 μm; Resolute or Integrity, ≥110 μm; Xience, ≥100 μm; and Nobori or Biomatrix, ≥130 μm.[15-19] The percent of malapposed or uncovered struts in each stented lesion was calculated as: (number of malapposed or uncovered struts/total number of struts in all cross-sections of the lesion)×100.[7]

Continuous data are presented as mean±standard deviation, and categorical data are presented as number (%). Pearson's two-way test was used to assess the relationships between two quantitative variables. Each pre-procedural plaque component (NC, DC, FT, and FF) was classified into quartiles.

Analysis of variance was used to compare the percentage of malapposed or uncovered struts according to each plaque component quartile. Multivariate analysis was performed to determine the independent predictors of late stent malapposition. Variables that reached a $p<0.1$ in univariate analysis were included in a multivariate forward stepwise regression analysis. Statistical analysis was performed with SPSS software, version 18.0 (SPSS Inc., Chicago, IL, USA), and a p-value <0.05 was considered statistically significant.

RESULTS

Clinical, procedural, and pre-procedural VH-IVUS characteristics according to the presence of late stent malapposition are summarized in Table 1 and 2. Follow-up OCT characteristics are summarized in Table 3. Pre-procedural absolute total NC and DC plaque volumes were positively correlated with the percentage of malapposed struts (r=0.44, $p<0.001$, Fig. 1A and r=0.45, $p<0.001$, Fig. 1B, respectively), and pre-procedural absolute total FT plaque volume was weakly associated with the percentage of malapposed struts (r=0.220, $p=0.015$). When each relative total plaque volume was classified into quartiles according to the plaque components, the highest NC plaque volume quartile and the highest DC plaque volume quartile had a significantly higher percentage of malapposed struts ($p=0.013$ for relative NC plaque volume, $p=0.020$ for relative DC plaque volume) (Fig. 2A). The highest FT plaque volume quartile had a lower percentage of malapposed struts ($p=0.040$). The lesions with stent malapposition on follow-up OCT had a

Table 1. Baseline Clinical and Procedural Characteristics

	Overall, n=121	Late stent malapposition (+), n=37	Late stent malapposition (-), n=84	*p* value
Age, yr	61±9	63±8	60±10	0.063
Male, n (%)	88 (73)	29 (78)	59 (70)	0.354
Clinical presentation, n (%)				0.205
Stable angina	78 (65)	27 (73)	51 (61)	
Unstable angina	25 (20)	4 (11)	21 (25)	
Non-ST elevation myocardial infarction	18 (15)	6 (16)	12 (14)	
Hypertension, n (%)	74 (61)	27 (73)	47 (56)	0.077
Diabetes mellitus, n (%)	42 (35)	11 (30)	31 (37)	0.445
Dyslipidemia, n (%)	67 (55)	27 (73)	40 (48)	0.010
Current smoker, n (%)	31 (26)	10 (27)	21 (25)	0.814
Target lesions, n (%)				0.357
Left anterior descending	73 (60)	22 (60)	51 (61)	
Left circumflex	20 (17)	4 (11)	16 (19)	
Right coronary artery	28 (23)	11 (30)	17 (20)	
Presence of thrombus on angiography	9 (7)	2 (5)	7 (8)	0.572
Reference vessel diameter, mm	3.1±0.5	3.3±0.4	3.0±0.5	0.024
Pre-procedural minimal lumen diameter, mm	1.2±0.4	1.3±0.5	1.1±0.3	0.136
Post-procedural minimal lumen diameter, mm	2.9±0.4	2.9±0.3	2.8±0.4	0.209
Post-procedural diameter stenosis, %	9.0±7.4	10.7±5.4	8.3±8.1	0.119
Follow-up minimal lumen diameter, mm	2.7±0.5	2.8±0.5	2.6±0.5	0.050
Follow-up diameter stenosis, %	9.9±13	7.7±11.9	10.9±12.7	0.192
Lesion length, mm	16.4±4.6	18.0±4.6	15.7±4.4	0.027
Plaque modification procedure	0	0	0	1.000
Stent diameter, mm	3.2±0.4	3.3±0.3	3.2±0.4	0.250
Stent length, mm	19.1±4.6	20.5±4.8	18.5±4.5	0.035
Stent type, n (%)				0.852
Sirolimus-eluting stent	36 (30)	12 (32)	24 (29)	
Zotarolimus-eluting stent	31 (26)	10 (27)	21(25)	
Everolimus-eluting stent	8 (7)	3 (8)	5 (6)	
Biolimus-eluting stent	46 (38)	12 (32)	34 (41)	
Post-dilation, n (%)	82 (68)	26 (70)	56 (67)	0.696
Maximal dilated pressure, atm	17.6±3.5			

http://dx.doi.org/10.3349/ymj.2015.56.6.1538

Table 2. Pre-Procedural VH-IVUS

	Total, n=121	Late stent malapposition (+), n=37	Late stent malapposition (-), n=84	*p* value
Pre-procedural gray-scale IVUS characteristics				
Target lesion CSA with minimum lumen area				
EEM CSA, mm^2	13.0±4.1	14.2±4.1	12.4±4.1	0.028
Lumen CSA, mm^2	2.7±0.9	3.2±1.2	2.5±0.6	0.003
P&M CSA, mm^2	10.2±4.0	11.0±3.8	9.9±4.0	0.139
Plaque burden, %	77.3±9.0	76.5±9.2	77.6±8.9	0.529
Pre-procedural VH-IVUS characteristics				
Absolute total plaque volume, mm^3				
Necrotic core	22.9±19.0	30.7±22.3	19.5±16.4	0.008
Dense calcium	7.9±9.6	12.3±14.5	5.9±5.4	0.012
Fibrotic	63.8±33.8	68.1±28.7	61.9±35.8	0.358
Fibrofatty	16.5±12.4	16.5±13.1	16.6±12.1	0.973
Relative total plaque volume, %				
Necrotic core	18.9±9.1	22.1±8.7	17.4±8.9	0.009
Dense calcium	6.7±5.1	8.6±5.9	5.9±4.5	0.008
Fibrotic	59.3±9.8	56.4±9.8	60.5±9.6	0.031
Fibrofatty	15.1±10.3	12.7±7.8	16.2±11.1	0.081

IVUS, intravascular ultrasound; EEM, external elastic membrane; CSA, cross-sectional area; P&M, plaque and media; VH, virtual histology.
Values were presented as mean±standard deviation.

significantly larger initial absolute total NC plaque volume (30.7±22.3 mm^3 vs. 19.5±16.4 mm^3, p=0.008) and absolute total DC plaque volume (12.3±14.5 mm^3 vs. 5.9±5.4 mm^3, p=0.012) (Table 2). Similarly, the lesions with stent malapposition had a significantly larger relative total NC plaque volume (22.1±8.7% vs. 17.4±8.9%, p=0.009) and a larger relative total DC plaque volume (8.6±5.9% vs. 5.9±4.5%, p=0.008) (Table 2). On the pre-procedural IVUS images, among the 37 lesions with late stent malapposition, superficial calcium was observed in 24 lesions (65%) and deep calcium was observed in eight lesions (21%). The remaining five lesions (14%) did not have calcium. Also, the mean calcium length of the 31 calcified lesions was 8.9±8.3 mm, and the proportion of calcium length with regard to total lesion length was 44±30%.

As for the percentage of uncovered struts, there was no significant relationship with absolute total NC plaque volume (r=0.11, p=0.227) (Fig. 1C) or absolute total DC plaque volume (r=0.15, p=0.102) (Fig. 1D). Similarly, there were no significant differences in the percentage of uncovered struts among the relative total volume quartiles of each plaque component (Fig. 2B).

On multivariate analyses, pre-procedural absolute total DC plaque volume was the only independent predictor of late stent malapposition (β=1.12, p=0.002).

DISCUSSION

The main findings of the present study were as follows: 1) pre-procedural quantitative assessment of plaque composition by VH-IVUS may predict the degree of late stent malapposition detected by OCT; 2) greater pre-procedural DC plaque burden was associated with greater late stent malapposition and was the only independent predictor for late stent malapposition; and 3) pre-procedural plaque composition was not associated with strut coverage on follow-up OCT after DES implantation.

Until now, there has been little data regarding the association between pre-procedural plaque composition evaluated by VH-IVUS and strut coverage on follow-up OCT after DES implantation. Even though plaque characteristics seem to strongly affect vascular healing responses after DES implantation, no data exists regarding the impact of plaque characteristics on late stent malapposition or coverage of struts, which may be considered potential risk factors for the occurrence of late stent thrombosis.[1-5] In addition, many previous OCT studies evaluating vascular responses after DES implantation have commonly been limited by a lack of information regarding pre-procedural plaque characteristics of *de novo* lesions.[16,17] Given this situation, we sought to investigate the impact of plaque characteristics of *de novo* lesions on vascular responses following DES implantation using pre-procedural VH-IVUS and follow-up OCT.

Mechanisms of late persistent malapposition have been proposed. Malapposition might be mediated partly by calcified lesions that do not allow for homogeneous stent expansion and could result in the lack of contact of stent struts with the vessel walls.[1] Also, as for plaque characteristics affecting the occurrence of stent malapposition, a recent OCT study re-

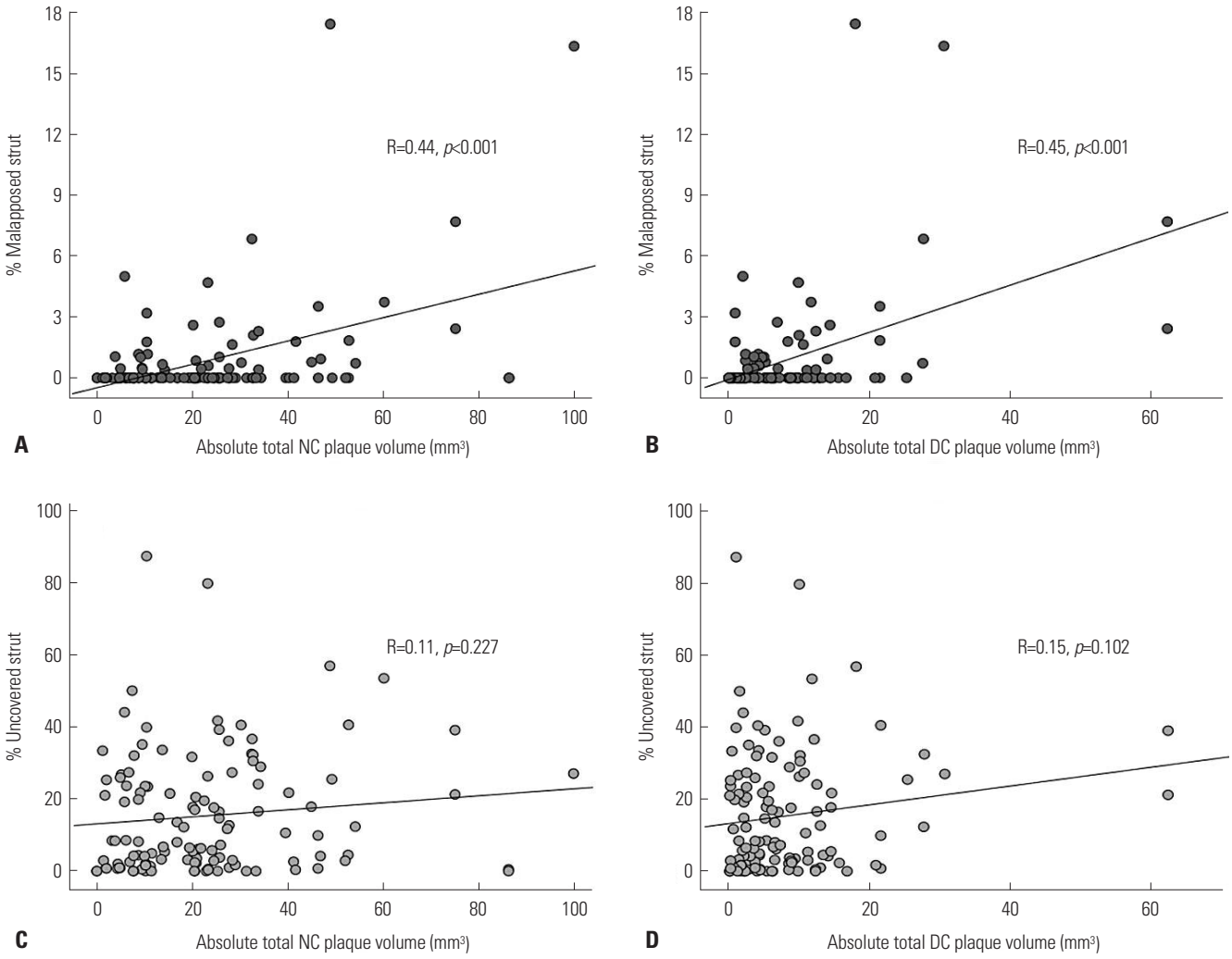

Fig. 1. Correlation between absolute total plaque component volumes and percentage of malapposed (A and B) or uncovered struts (C and D) on follow-up OCT. Absolute total NC plaque volume and absolute total DC plaque volume were positively correlated with percentage of malapposed struts but not with percentage of uncovered struts. OCT, optical coherence tomography; NC, necrotic core; DC, dense calcium.

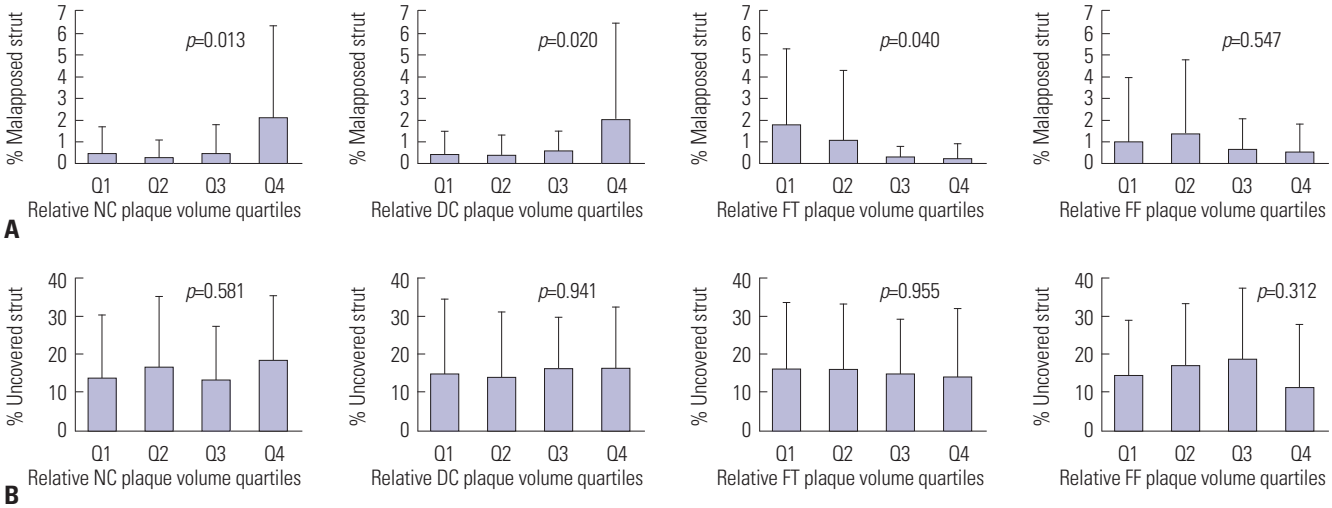

Fig. 2. Percentage of malapposed (A) and uncovered struts (B) according to the relative total plaque volume quartiles of each plaque component. The highest relative NC plaque volume quartiles and the highest relative DC plaque volume quartiles had a significantly higher percentage of malapposed struts. NC, necrotic core; DC, dense calcium; FT, fibrotic; FF, fibrofatty.

http://dx.doi.org/10.3349/ymj.2015.56.6.1538

Table 3. Pre-Procedural VH-IVUS and Matched Follow-Up OCT Characteristics

Follow-up OCT characteristics	Total, n=121
Time interval to follow-up OCT, months	6.3±3.1
Total mean number of cross sections, n	17.2±5.0
Total mean number of analyzable struts, n	189±58
Mean stent CSA, mm^2	7.5±2.0
Mean lumen CSA, mm^2	7.0±2.0
Mean NIH CSA, mm^2	0.5±0.4
Percentage of NIH CSA, %	6.5±5.3
Median NIH thickness, μm	54.5 (35.1–96.3)*
Percent malapposed struts, %	0.8±2.5
Percent uncovered struts, %	15.3±16.7
Percentage of both of malapposed and uncovered struts, %	0.5±1.8
Cross sections with any uncovered strut, %	31.1±37.6
Cross sections with a ratio of uncovered to total strut >0.3, %	15.4±26.9
Cross sections with any malapposed strut, %	3.0±9.5
Stent malapposition, n (%)	37 (31)

OCT, optical coherence tomography; CSA, cross-sectional area; NIH, neointimal hyperplasia; VH-IVUS, virtual histology intravascular ultrasound.
*Was presented as median (interquartile range).

ported that the presence of calcium was one independent predictor of late persistent stent malapposition after DES implantation.[6] Therefore, although we could not classify late stent malapposition into late-acquired and persistent malapposition in the present study, larger DC volumes may be important for late persistent stent malapposition. Other IVUS studies have suggested that late-acquired stent malapposition occurs mainly due to positive remodeling and plaque/thrombus resolution.[20,21] In the present study, we found that absolute total NC plaque volume is also positively related to the degree of late stent malapposition in univariate analysis. Thus, larger NC volumes may be important for late-acquired stent malapposition. Similar to our study, a previous study reported that a post-stented NC component was associated with the development of late stent malapposition on follow-up IVUS after DES implantation, particularly in patients with acute myocardial infarction and diabetes mellitus.[22] However, the present study is different from the previous study in that we assessed the plaque characteristics pre-intervention, not post-intervention. Furthermore, we assessed vascular healing responses using OCT, not IVUS, which might weight the importance of this study. Our study showed that pre-procedural plaque composition may play an essential role in formation of late stent malapposition after DES implantation.

Late stent thrombosis after DES implantation is a serious concern because of delayed vascular healing and inflammatory reaction. Uncovered struts on follow-up OCT have been proposed as potential risk factors for late stent thrombosis after DES implantation.[4,5] A previous study showed that coverage of malapposed stent segments is delayed, compared to well-apposed segments, and that the larger the acute malapposition, the greater the likelihood of persistent malapposition and delayed healing at follow-up.[4] Thus, we hypothesized that plaque composition, particularly a DC or NC component, may result in delayed strut coverage. However, in the present study, there were no significant associations between the specific plaque components and strut coverage after DES implantation. Considering the results of our previous OCT study, DES type rather than plaque characteristics on VH-IVUS may be the more powerful factor in determining strut coverage.[7]

This study has several limitations. First, it was not clear whether the malappositions at follow-up were residual or newly acquired because post-procedural intravascular imaging studies were not preformed immediately after DES implantation. Second, this study was based on registry data, and the sample size was quite small. Finally, different types of DES were used.

In conclusion, pre-procedural assessment of plaque composition by VH-IVUS may predict the formation of late stent malapposition detected by OCT at follow-up. Larger pre-procedural DC plaque volumes were associated with late stent malapposition. However, pre-procedural plaque composition was not associated with decreased strut coverage at follow-up after DES implantation.

ACKNOWLEDGEMENTS

This study was supported by a grant from the Korea Healthcare Technology R&D Project, Ministry for Health, Welfare & Family Affairs, Republic of Korea (No. A085012 and A102064); a grant from the Korea Health 21 R&D Project, Ministry of Health & Welfare, Republic of Korea (No. A085136); and the Cardiovascular Research Center, Seoul, Korea.

REFERENCES

1. Cook S, Wenaweser P, Togni M, Billinger M, Morger C, Seiler C, et al. Incomplete stent apposition and very late stent thrombosis after drug-eluting stent implantation. Circulation 2007;115:2426-34.
2. Siqueira DA, Abizaid AA, Costa Jde R, Feres F, Mattos LA, Staico R, et al. Late incomplete apposition after drug-eluting stent implantation: incidence and potential for adverse clinical outcomes. Eur Heart J 2007;28:1304-9.
3. Hassan AK, Bergheanu SC, Stijnen T, van der Hoeven BL, Snoep JD, Plevier JW, et al. Late stent malapposition risk is higher after drug-eluting stent compared with bare-metal stent implantation and associates with late stent thrombosis. Eur Heart J 2010;31:1172-80.
4. Guagliumi G, Sirbu V, Musumeci G, Gerber R, Biondi-Zoccai G, Ikejima H, et al. Examination of the in vivo mechanisms of late drug-eluting stent thrombosis: findings from optical coherence tomography and intravascular ultrasound imaging. JACC Cardiovasc Interv 2012;5:12-20.
5. Won H, Shin DH, Kim BK, Mintz GS, Kim JS, Ko YG, et al. Optical

coherence tomography derived cut-off value of uncovered stent struts to predict adverse clinical outcomes after drug-eluting stent implantation. Int J Cardiovasc Imaging 2013;29:1255-63.
6. Im E, Kim BK, Ko YG, Shin DH, Kim JS, Choi D, et al. Incidences, predictors, and clinical outcomes of acute and late stent malapposition detected by optical coherence tomography after drug-eluting stent implantation. Circ Cardiovasc Interv 2014;7:88-96.
7. Kim BK, Kim JS, Oh C, Ko YG, Choi D, Jang Y, et al. Major determinants for the uncovered stent struts on optical coherence tomography after drug-eluting stent implantation. Int J Cardiovasc Imaging 2012;28:705-14.
8. Guo N, Maehara A, Mintz GS, He Y, Xu K, Wu X, et al. Incidence, mechanisms, predictors, and clinical impact of acute and late stent malapposition after primary intervention in patients with acute myocardial infarction: an intravascular ultrasound substudy of the Harmonizing Outcomes with Revascularization and Stents in Acute Myocardial Infarction (HORIZONS-AMI) trial. Circulation 2010;122:1077-84.
9. Gutiérrez-Chico JL, Wykrzykowska J, Nüesch E, van Geuns RJ, Koch KT, Koolen JJ, et al. Vascular tissue reaction to acute malapposition in human coronary arteries: sequential assessment with optical coherence tomography. Circ Cardiovasc Interv 2012;5:20-9, S1-8.
10. Ozaki Y, Okumura M, Ismail TF, Naruse H, Hattori K, Kan S, et al. The fate of incomplete stent apposition with drug-eluting stents: an optical coherence tomography-based natural history study. Eur Heart J 2010;31:1470-6.
11. Mintz GS, Nissen SE, Anderson WD, Bailey SR, Erbel R, Fitzgerald PJ, et al. American College of Cardiology Clinical Expert Consensus Document on Standards for Acquisition, Measurement and Reporting of Intravascular Ultrasound Studies (IVUS). A report of the American College of Cardiology Task Force on Clinical Expert Consensus Documents. J Am Coll Cardiol 2001;37:1478-92.
12. Nair A, Kuban BD, Tuzcu EM, Schoenhagen P, Nissen SE, Vince DG. Coronary plaque classification with intravascular ultrasound radiofrequency data analysis. Circulation 2002;106:2200-6.
13. Nasu K, Tsuchikane E, Katoh O, Vince DG, Virmani R, Surmely JF, et al. Accuracy of in vivo coronary plaque morphology assessment: a validation study of in vivo virtual histology compared with in vitro histopathology. J Am Coll Cardiol 2006;47:2405-12.
14. Takano M, Inami S, Jang IK, Yamamoto M, Murakami D, Seimiya K, et al. Evaluation by optical coherence tomography of neointimal coverage of sirolimus-eluting stent three months after implantation. Am J Cardiol 2007;99:1033-8.
15. Barlis P, Dimopoulos K, Tanigawa J, Dzielicka E, Ferrante G, Del Furia F, et al. Quantitative analysis of intracoronary optical coherence tomography measurements of stent strut apposition and tissue coverage. Int J Cardiol 2010;141:151-6.
16. Kim BK, Hong MK, Shin DH, Kim JS, Ko YG, Choi D, et al. Optical coherence tomography analysis of strut coverage in biolimus- and sirolimus-eluting stents: 3-month and 12-month serial follow-up. Int J Cardiol 2013;168:4617-23.
17. Kim BK, Ha J, Mintz GS, Kim JS, Shin DH, Ko YG, et al. Randomised comparison of strut coverage between Nobori biolimus-eluting and sirolimus-eluting stents: an optical coherence tomography analysis. EuroIntervention 2014;9:1389-97.
18. Tanigawa J, Barlis P, Dimopoulos K, Dalby M, Moore P, Di Mario C. The influence of strut thickness and cell design on immediate apposition of drug-eluting stents assessed by optical coherence tomography. Int J Cardiol 2009;134:180-8.
19. Davlouros PA, Mavronasiou E, Xanthopoulou I, Karantalis V, Tsigkas G, Hahalis G, et al. An optical coherence tomography study of two new generation stents with biodegradable polymer carrier, eluting paclitaxel vs. biolimus-A9. Int J Cardiol 2012;157:341-6.
20. Hong MK, Mintz GS, Lee CW, Park DW, Park KM, Lee BK, et al. Late stent malapposition after drug-eluting stent implantation: an intravascular ultrasound analysis with long-term follow-up. Circulation 2006;113:414-9.
21. Ako J, Morino Y, Honda Y, Hassan A, Sonoda S, Yock PG, et al. Late incomplete stent apposition after sirolimus-eluting stent implantation: a serial intravascular ultrasound analysis. J Am Coll Cardiol 2005;46:1002-5.
22. Hong YJ, Jeong MH, Choi YH, Song JA, Jang SY, Yoo JH, et al. Relation between poststenting peristent plaque components and late stent malapposition after drug-eluting stent implantation: virtual histology-intravascular ultrasound analysis. Int J Cardiol 2013;167:1882-7.

http://dx.doi.org/10.3349/ymj.2015.56.6.1538